RSC Advances

PAPER

View Article Online
View Journal | View Issue



Cite this: *RSC Adv.*, 2020, **10**, 31049

# A novel π-conjugated poly(biphenyl diimide) with full utilization of carbonyls as a highly stable organic electrode for Li-ion batteries†

Zhijun Wang,[a] Bingjie Zhang,[a] Yueyan Zhang,[a] Ni Yan [b] and Gang He *[a]

Received 22nd June 2020
Accepted 29th July 2020

DOI: 10.1039/d0ra05483f

rsc.li/rsc-advances

Organic carbonyl redox polymers, especially conjugated polyimides with multiple reversible redox centers have attracted considerable attention as electrode materials for organic Li-ion batteries. However, the low utilization of carbonyls hindered their potential applications in energy storage. Herein, a novel π-conjugated polyimide (**PBPI**) based on biphenyl diimide (**BPI**) containing two seven-membered imide rings is developed. **PBPI** is used as an anode material for organic Li-ion batteries, which show high conductivity and insolubility in the electrolyte and enable intercalation of four Li-ions per **BPI** unit, thus contributing to a reversible capacity of 136 mA h $g^{-1}$ at 100 mA $g^{-1}$ with coulombic efficiency close to 100%. Moreover, the battery based on **PBPI** manifested superior high-rate performance (65 mA h $g^{-1}$ at 2000 mA $g^{-1}$) as well as significant cycling stability (over 1600 cycles at 100 mA $g^{-1}$). Remarkably, the full redox-active site (C=O) utilization of an aromatic diimide core to achieve its full potential applications is reported for the first time. This work provides a new strategy for developing redox π-conjugated polyimides and accommodation of more alkaline ions for high performance battery systems.

## 1. Introduction

Organic rechargeable batteries are excellent candidates for next-generation energy storage systems due to the advantage of high theoretical specific capacity, abundant raw materials, low cost, easy processing, system security as well as being eco-friendly.[1–8] Over the past decades, different types of organic materials with various redox centers or molecular structures have been exploited as electrodes in rechargeable battery systems.[9–17] However, their widespread development is limited by intrinsic problems such as poor electronic conductivity, easy dissolution into liquid electrolytes, and low volumetric energy density. Recently, various organic electrode materials including polymer,[18,19] organosulfur compounds,[20,21] radical polymers,[22,23] and carbonyl compounds[24–26] have been extensively exploited. Among these, organic carbonyl compounds have received much attention due to being metal-free, low-cost, environmentally friendly, and flexibility.[27] Additionally, amidst all kinds of organic carbonyl compounds, polyimides represent the most promising electrode materials because of their structural characteristics of multi-carbonyls conjugated with the aromatic core and the fused cyclic imide.[28–31] Recent years, lots of polyimides have been investigated as electrode materials in energy storage application.[32–37] However, these polymers are connected *via* nitrogen atoms and form a tertiary amine structure, which affect the life of the battery. Meanwhile, the above-mentioned polyimide materials generally prefer to be applied as cathodes rather than anodes owing to their relatively high redox potentials (typically 1.5–4.0 V *vs.* $Li^+/Li$). Though several conjugated polyimides as cathode electrodes have been developed with good performance,[38–40] but they still suffer from the dissolution problem and cannot obtain satisfactory cycling performance.[35] Thus, it's very urgent to design novel organic anode materials with significant cyclic stability and high capacity. The most crucial factor of cycling stability is the solubility of the active material in the electrolyte because the dissolution of active materials will lead to a decrease of the capacity. An efficient strategy to solve the dissolution problem and improve the cycling stability is to construct polyimides with a stable skeleton since they are always completely insoluble in battery electrolytes. However, it is widely accepted that polymerization will sacrifice theoretical capacity, enlarge electrochemical polarization, and hinder ion/electron transportation.[4] To overcome the drawback of low electrical conductivity, the polymer structure could be incorporated with a large conjugated system, which is beneficial to the charge transfer.[2] Theoretically, the larger number of the reactive carbonyl group, the higher specific capacity of the material will be. However, the main challenge of those polyimide electrodes for organic Li-ion batteries lies in the deficient redox-active site

[a]*Frontier Institute of Science and Technology, State Key Laboratory for Strength and Vibration of Mechanical Structures, Xi'an Key Laboratory of Sustainable Energy Materials Chemistry, Xi'an Jiaotong University, Xi'an, Shaanxi Province, 710054, China. E-mail: ganghe@mail.xjtu.edu.cn*

[b]*Polymer Materials and Engineering Department, Institute of Polymer Materials, School of Materials Science and Engineering, Chang'an University, Xi'an, 710064, China*

† Electronic supplementary information (ESI) available. See DOI: 10.1039/d0ra05483f

(C═O) utilization especially during long-term operations at high current densities.[27] According to previous reports, there is a drawback with the electrochemical reduction of polyimide electrodes that the full capacity may be obtained at a deeper discharge with four-electron transfer below 1.5 V while accompanied by serious structural damage and irreversible decomposition.[28] One way to increase the capacity is to fully utilize the redox sites of the imide core for Li insertion. By adjusting and controlling the structure of the aromatic imide unit, the full utilization of redox-active sites (C═O) of polyimide electrodes could be achieved for better capacity performance.[27]

Based on these considerations of the chemical structures and potential application, herein, we designed and synthesized a novel conjugated polyimide (**PBPI**) (Scheme 1) containing biphenyl diimide building block, 2,6-dibromobiphenyldiimide (**BPI**) with two seven-membered rings conjugated with bithiophene. Remarkably, the **PBPI** possesses obvious advantages such as unique redox properties, high conjugation and being insoluble in aprotic electrolyte. When used as an anode material for organic Li-ion batteries, PPBI showed a low voltage potential of 1.1 V, a high initial discharge capacity, superior high-rate performance as well as significant cyclic stability (over 1600 cycles). Based on density functional theory (DFT) calculations and experimental investigations, the lithiation mechanism of **PBPI** is proved to be a four-electron redox process for each diimide unit. Thus, the full potential application of redox-active site (C═O) as electrodes for organic Li-ion batteries was presented.

## 2. Experimental

### 2.1. Materials characterization

NMR spectra were measured on a Bruker Avance-400 spectrometer in the solvents indicated; chemical shifts are reported in units (ppm) by assigning TMS resonance in the $^{1}H$ spectrum as 0.00 ppm, $CDCl_3$ resonance in the $^{13}C$ spectrum as 77.0 ppm. UV-vis measurements were performed using DH-2000-BAL Scan spectrophotometer. Fluorescence measurements were performed at room temperature on a time-correlated single photon counting Edinburgh FLS 920 fluorescence spectrometer. TGA measurements were conducted on a TGA Q500 instruments under a dry nitrogen flow at a heating rate of 10 °C $min^{-1}$, heating from room temperature to 600 °C. DSC analyses were performed on a DSC Q2000 instruments under a dry nitrogen flow at a heating rate of 10 °C $min^{-1}$, heating from −30 °C to 300 °C. Electrochemical measurements was carried out on a CHI610D instruments in a conventional three-electrode cell with a gold working electrode, a platinum wire counter electrode, and a Ag/AgCl reference electrode. GPC measurements were made using a GPC 270 Max instrument equipped with a Viscotek VE 2001 plus autosampler, three μ-Styragel columns, and a Viscotek VE 3580 refractive index (RI) detector. The columns were calibrated using polystyrene standards. Cyclic voltammetry was conducted in an Ar-filled glove box with oxygen and water content lower than 0.1 ppm. Three-electrode configuration was adopted where a gold plate was used as working electrode, a platinum mesh was used as counter electrode, and Ag/AgCl filled with electrolyte was used as reference electrode in 0.10 M $Bu_4NPF_6$ solution in degassed and dried THF. The scan rate is 50 mV $s^{-1}$. Potentials are determined against a ferrocene/ferrocenyl ion couple ($Fc/Fc^{+}$).

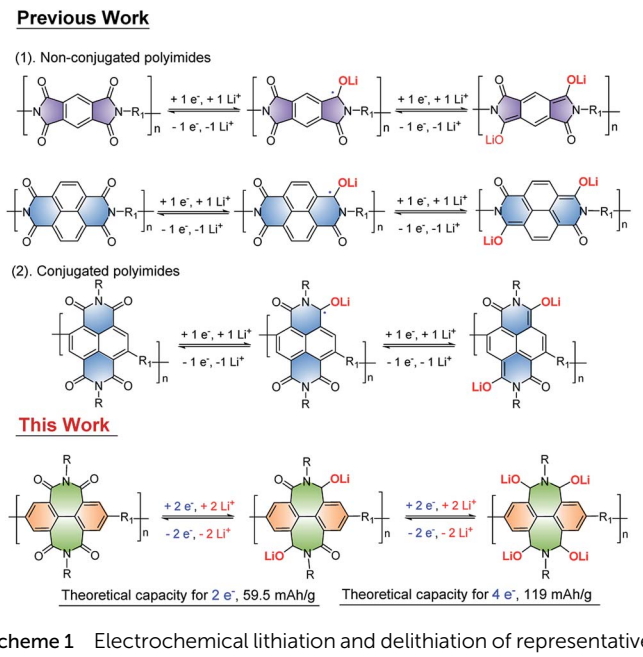


Scheme 1 Electrochemical lithiation and delithiation of representative polyimides and PBPI.

### 2.2. Electrode preparation and battery fabrication

The battery electrode was prepared by conventional slurry coating method where active material: carbon black: PVDF = 6 : 3 : 1, 30 mg of mixed powder was grounded and stirred in 0.5 mL mixture of NMP to form a viscous slurry. The slurry was then coated on copper foil with a doctor blade. The slurry was then coated on copper foil with a doctor blade. The electrodes were dried in vacuum at 80 °C for 8 h and then punched into round disks with diameter of 12 mm. The active material loading on copper current collector was about 1 mg $cm^{-2}$. The Li-ion battery was assembled in CR2032 coin cell in an Ar-filled glove box with oxygen and water content lower than 0.1 ppm. Lithium plate with diameter of 12 mm and thickness of 1 mm was used as both counter and reference electrode; a piece of glass fiber (diameter = 16 mm) was used as separator, and 100 μL 1 M lithium hexafluorophosphate in ethylene carbonate/dimethyl carbonate/ethyl methyl carbonate (1 : 1 : 1 vol%) was used as electrolyte for each cell.

### 2.3. Electrochemical measurement

Galvanostatic charge–discharge cycles were conducted on a LAND CT2001A battery tester at different current densities in the voltage range from 0.5 V to 3.0 V. The cyclic voltammetry was measured by using an Ametek PARSTAT4000 electrochemistry workstation between 0.5 V and 3.0 V (*vs.* $Li/Li^{+}$) at a constant scanning rate of 0.1–1.0 mV $s^{-1}$. Electrochemical impedance spectroscopy (EIS) studies were carried out on the same electrochemistry workstation by applying a perturbation voltage of

 

10 mV in a frequency range of 100 kHz to 10 mHz. The surface morphology was observed by scanning electron microscope (SEM, Sirion, 2000, FEI).

# 3. Results and discussion

## 3.1. Synthesis

The structures and synthetic routes of the new diimide **BPI** and polyimide **PBPI** were illustrated in Scheme 2. The **BPI** monomer was synthesized according to our previous work.[41] The **PBPI** was synthesized *via* ($Pd_2(dba)_3$/P(*o*-tolyl)$_3$)-catalyzed stille type-coupling reactions.[42] The detailed procedures and characterization data were shown in the ESI.† The molecular weight of the polymer was measured by GPC at 150 °C using trichlorobenzene as the eluent and the number-average molecular weight (Mn) is 20.3 kD. (Table S1†).

## 3.2. Thermal stabilities, photophysical and electrochemical properties

Thermogravimetric analysis (TGA) measurements were implemented, and the results demonstrated that **PBPI** was thermally stable with onset decomposition temperatures of 327 °C (Fig. S1a†). Meanwhile, differential scanning calorimetry (DSC) was also measured (Fig. S1b†). **PBPI** shown no phase transition due to its high thermal stability. The large molecular weights and good thermal stability of the polyimide demonstrated the potential of applying it as active electrochemical materials in organic rechargeable batteries. The UV-vis spectra of **PBPI** in DCM and in thin film were also investigated. As shown in Fig. S2a,† **PBPI** exhibited main characteristic absorption bands at about 469 nm in DCM with an absorption shoulder, which was similar to the vibronic profiles reported in regular polythiophene spectra.[43] Although the maximum of absorption spectrum of **PBPI** film was almost the same with in DCM, the onsets of the spectrum were red-shifted (band gap in films: 2.41 eV for **PBPI**, Fig. S2b†), which was also found in previous reported BTI-containing polymers. The results can be ascribed to the twisted **BPI**-containing rigid polymer backbones and probable pre-aggregation in solution.[44] The fluorescence spectra of **PBPI** in DCM and in film state were shown in Fig. S3,† the emission peaks ($\lambda_{em}$) of **PBPI** were centred at 489 nm in DCM and 558 nm in the film state, showing a red-shift from solution to film state, which was a common phenomenon for conjugated polymers owing to the molecular organization in films to form more ordered structures leading to the stronger aggregation.[45] Cyclic voltammetry (CV) was carried out to determine the LUMO energy level and study the redox properties of **BPI**-based polymer. As shown in Fig. S4,† **PBPI** presented two weak reduction peaks and one weak symmetrical oxidation peak, and the LUMO level was −2.81 eV, which was consistent with the DFT calculations (deviations of about 0.7 eV).

## 3.3. Electrochemical properties

The electrochemical performance of **PBPI** has been studied *versus* Li/Li$^+$ by employing cyclic voltammetry (CV) at different scan rates from 0.1 to 1.0 mV s$^{-1}$ in the coin-type battery test (Fig. 1a). The two reduction peaks were all below 1.5 V shown in the CV curves, which were the same as those in the galvanostatic charge–discharge test. The electrochemical properties of **PBPI** were also investigated as an electrode material in Li/**PBPI** half-cells carried out at a current density of 200 mA g$^{-1}$ and in the potential range of 0.5–3.0 V. As shown in Fig. 1b, **PBPI** displayed a specific capacity of 136 mA h g$^{-1}$ in the second cycle, which was a 110% of the theoretical specific capacity of 119 mA h g$^{-1}$ based on a four-electron transfer process at the **BPI** unit. The capacity exceeding 100% may attribute to the contribution of carbon black.[46] The sloping charge–discharge voltage profiles were attributed to the Li-ions insertion into polymers of different molecular weight and phase domains at different voltages.

The rate capability of electrode materials is related to the electron- and ion-transfer rates of the redox reaction. The **PBPI** electrode can deliver a discharge capacity of 135, 107, 94, 81, 71 and 65 mA h g$^{-1}$ at current densities of 50, 100, 200, 500, 1000 and 2000 mA g$^{-1}$, respectively (Fig. 2a). After 36 cycles, the current density was reduced to the starting value (50 mA g$^{-1}$) and a high reversible capacity of 95 mA h g$^{-1}$ was recovered, which demonstrated the high-rate capability and structural stability of the **PBPI** electrode. We speculated that this is credited to the high electron mobility in its extended conjugated ring system as well as the submicrometer size feature of the particles. The **PBPI** electrode also exhibited excellent cycling performance at a current density of 100 mA g$^{-1}$ (Fig. 2b). After

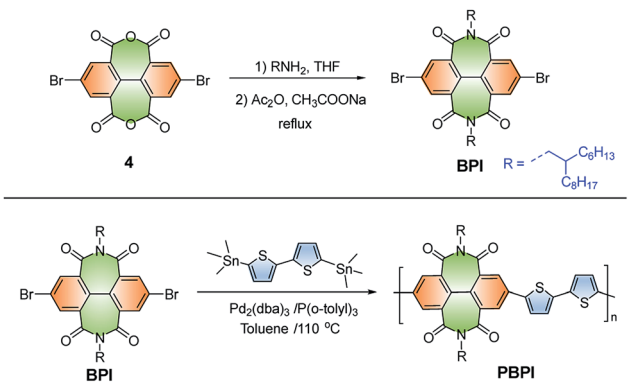


Scheme 2 Synthesis of the conjugated polyimide (PBPI).

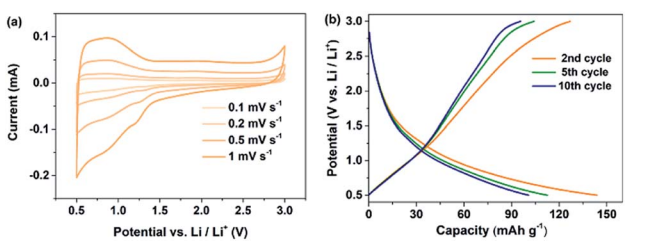


Fig. 1 (a) Cyclic voltammograms of PBPI in the potential range of 0.5–3 V (*vs.* Li/Li$^+$) at a rate of 0.1–1 mV s$^{-1}$. (b) galvanostatic discharge/charge profiles of PBPI at a current density of 100 mA g$^{-1}$.

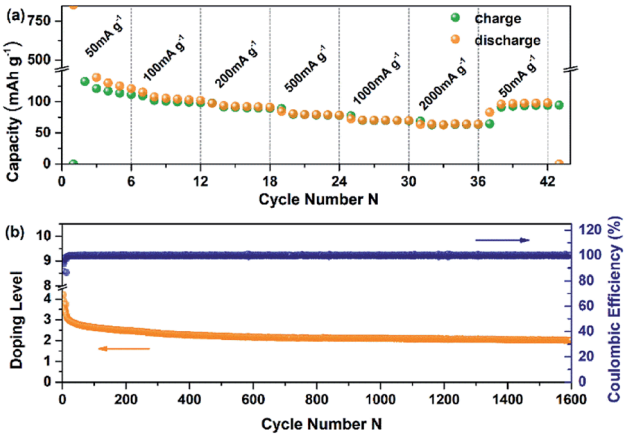


Fig. 2 (a) Rate capability at various current densities. (b) Reversibility of PBPI during repeated deep doping–undoping at 100 mA $g^{-1}$.

the first 10 cycles, **PBPI** electrode retained doping level of around 3.4 and 2.1 after 1600 cycles, which corresponded to more than half of the theoretical value based on a four-electrons redox process at the **BPI** unit. After 10 cycles, the coulombic efficiency of **PBPI** was over 98%, suggesting that the number of insertion/desertion Li-ions in each cycle was mostly equivalent. This cycling stability was attributed to careful design of the conjugated polymer backbone to improve the conductivity, decrease the solubility in the electrolyte and maintain the mechanical integrity of the polymer electrode. In addition, to demonstrate the practical applications of **PBPI** electrode, a packaged flexible cell was fabricated. As demonstrated in Fig. S6,† the light-emitting diode (LED) can be easily lightened under the flat and bending states. More importantly, the flexible cell showed good capacity and repeatability, thus clearly demonstrating that this battery based on **PBPI** electrode not only show higher capacity and cycle stability, but also possess good flexibility.

The solubility of **PBPI** in the electrolyte was tested. After polymerization, the polymer became less dissolvable in the electrolyte. As showed in Fig. S7,† the colour of the electrolyte was nearly invariable when **PBPI** was soaked in the electrolyte for 5 days, which means that the **PBPI** material tends to stabilize after the molecules with lower degree of polymerization are dissolved. We also investigated the UV-vis spectra of lithium hexafluorophosphate solution and we found that there is little change of the UV-vis spectrum of the lithium hexafluorophosphate solution with the **PBPI** electrode soaked in for several days. Therefore, we speculated that the loss of specific capacity during the initial 10 cycles is due to the dissolution of the copolymer with low molecular weight in the electrolyte. After 10 cycles, the specific capacity become more stable. In order to explore the stability of **PBPI** electrode, the morphologies of the electrode materials have been investigated by scanning electron microscopy (SEM). As shown in Fig. 3a, the tiny spherical particles of **PBPI** and acetylene black were uniformly distributed after ball milling with the average size of 50–100 nm. The particle sizes and the compatibilities of

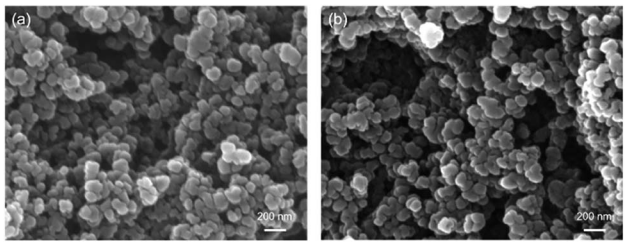


Fig. 3 SEM images of electrode materials (a) before and (b) after 100 cycles at 100 mA h $g^{-1}$.

carbonyl compounds and carbon black in the blend have a significant impact on the batteries' capacity and stability. The smaller size of the particles provides greater effective surface area thus enables faster and more reversible transfer of Li-ions.[47] We also investigated the BET test diagram, and the specific area was 28.677 $m^2$ $g^{-1}$. Fig. 3b showed the SEM images of the electrode after 100 cycles at 100 mA h $g^{-1}$. There was comparatively little change in morphology, and no structural damages or collapses. It further illustrated the remarkable stability of the polymer and fully displayed the advantage of the **PBPI** used as a prospective anode material for organic Li-ion batteries.

To understand the capacitive and diffusive behaviour, we further investigated the electrode reaction kinetics of **PBPI** by electrochemical impendence spectroscopy (EIS). Fig. 4 and S8† showed the EIS evolution of **PBPI** electrode at different charge/discharge cycles. **PBPI** presented relatively low $R_\Omega$ (3.5 Ω) and $R_{ct}$ (33 Ω) according to the equivalent circuit model, which was the lowest $R_{ct}$ value of the polyimide-based electrode reported in the literature.[26,38] The interface resistance of **PBPI** electrode, represented by the depressed semicircle, increased from ~30 to ~80 Ω after five cycles and then stabilized at ~80 Ω during subsequent cycles. The low $R_{ct}$ values implied the **PBPI** electrode has high stability and reversibility during the lithiation/(de) lithiation process with faster charge-transfer kinetics and electrical responses.[48]

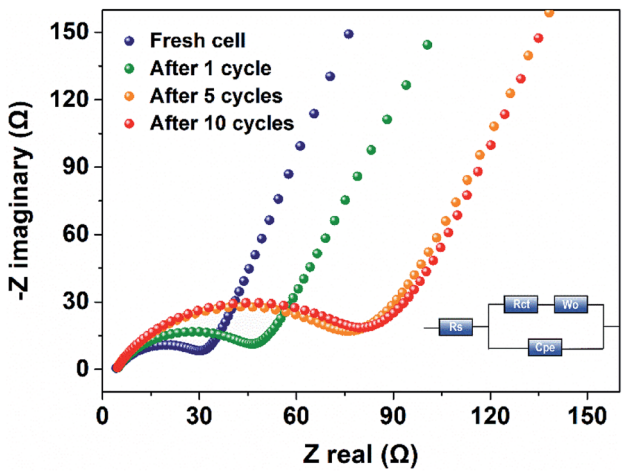


Fig. 4 EIS analysis of PBPI electrode.

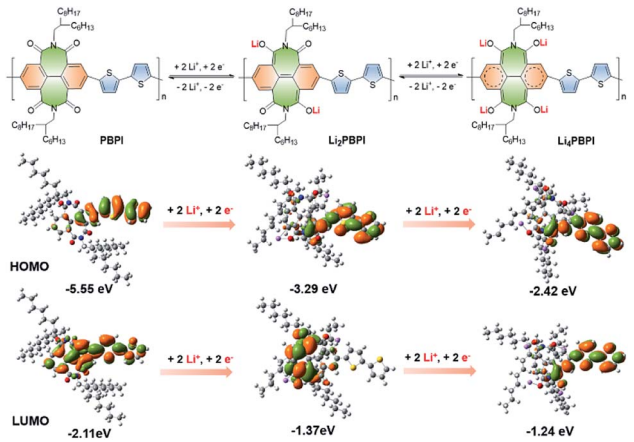


Fig. 5 Redox mechanism of **PBPI** and calculated LUMO and HOMO plots of **BPI** unit with different amounts of inserted-lithium.

To obtain a deeper insight into the reduction process, theoretical calculations were performed by using density functional theory (DFT). The redox structures revealed that the Li-ions were closely bonded with two or four carbonyl groups, contributing to the exceedingly low voltage of the **PBPI** and the high stability after lithiation. Theoretically, higher HOMO energy means lower ionization potential (IP) and better reducibility. Correspondingly, lower LUMO energy means better electron affinity (EA) and oxidizability. Beyond that, the narrow LUMO–HOMO gap ($E_g$) is related to good electronic conductivity.[42] According to the calculation result, the IP value and $E_g$ value of **PBPI** became smaller along with the insertion of Li-ions, demonstrating a higher redox activity and electronic conductivity after the insertion of Li-ions, which facilitated the two-step redox process. As shown in Fig. 5, the **BPI** unit has a LUMO energy of −2.11 eV, and the insertion of two Li-ions raised the LUMO energy up to −1.37 eV. After the insertion of four Li-ions, the LUMO energy of $Li_4$**PBPI** was raised up to −1.24 eV, much higher than that of Li (−1.52 eV), indicating difficulties for electrons to further transfer from Li atom to $Li_4$**PBPI**. This result confirmed that our initial structure design strategy of introducing twisted seven-membered cycles with carbonyl groups reduced the plateau potentials upon charge/discharge process, resulting a stable and reversible redox reaction in low redox potential and deliver an excellent rate capability. Clearly, **PBPI** was a very promising electrode material of organic Li-ion batteries.

## 4. Conclusions

In conclusion, a novel conjugated polyimide (**PBPI**) based on 2,6-disbrombiphenyl diimide (**BPI**) containing two seven-membered imide rings was synthesized and used as the anode material in organic Li-ion batteries for the first time. The polyimide with unparalleled structure showed excellent thermostabilities, strong emission in visible region both in solution and solid states and good redox activities. Additionally, the novel twisted seven-membered-ring structure combined with the extended conjugated skeleton solved the problems of poor conductivity and easy dissolution in the electrolyte to improve the batteries' capacity and stability. The Li-ion battery based on conjugated polyimide **PBPI** showed a specific capacity of 136 mA h $g^{-1}$ at the current density of 100 mA $g^{-1}$, superior rate performance and long cycle life (more than 1600 cycles). The experimental results and DFT calculations indicated a four-electron lithiation process for each repeat unit when working in the potential range of 0.5–3.0 V *vs.* $Li/Li^+$, which overcame the main challenge of deficient redox site utilization for conventional polyimides. This work demonstrated that the novel two seven-membered imide rings-containing polyimide was very promising material in energy storage applications.

## Conflicts of interest

There are no conflicts to declare.

## Acknowledgements

We gratefully acknowledge financial support from the Natural Science Foundation of China (21603016, 21704081, 21875180), Natural Science Foundation of Shaanxi province (2017JQ2023, 2018JM2026), the Cyrus Chung Ying Tang Foundation\o "gs4:". We also thank Prof. Yu Fang and Prof. Jun Liu for help discussion. We thank Dr Gang Chang and Yu Wang at Instrument Analysis Center of Xi'an Jiaotong University for their assistance with HRMS and Elemental analysis and photoluminescence (PL) spectra.

## Notes and references

1 Y. Liang, Z. Tao and J. Chen, Organic Electrode Materials for Rechargeable Lithium Batteries, *Adv. Energy Mater.*, 2012, **2**, 742–769.
2 C. Wang, Y. Xu, Y. Fang, M. Zhou, L. Liang, S. Singh, H. Zhao, A. Schober and Y. Lei, Extended pi-conjugated system for fast-charge and -discharge sodium-ion batteries, *J. Am. Chem. Soc.*, 2015, **137**, 3124–3130.
3 M. Stolar, C. Reus and T. Baumgartner, Xylene-Bridged Phosphaviologen Oligomers and Polymers as High-Performance Electrode-Modifiers for Li-Ion Batteries, *Adv. Energy Mater.*, 2016, **6**, 1600944.
4 S. Lee, G. Kwon, K. Ku, K. Yoon, S. K. Jung, H. D. Lim and K. Kang, Recent Progress in Organic Electrodes for Li and Na Rechargeable Batteries, *Adv. Mater.*, 2018, 1704682.
5 R. Mo, D. Rooney, K. Sun and H. Y. Yang, 3D nitrogen-doped graphene foam with encapsulated germanium/nitrogen-doped graphene yolk-shell nanoarchitecture for high-performance flexible Li-ion battery, *Nat. Commun.*, 2017, **8**, 13949.
6 N. Mohamed and N. K. Allam, Recent advances in the design of cathode materials for Li-ion batteries, *RSC Adv.*, 2020, **10**, 21662–21685.
7 W. Zhao, X. Mu, P. He and H. Zhou, Advances and Challenges for Aprotic Lithium-Oxygen Batteries using Redox Mediators, *Batteries Supercaps*, 2019, **2**, 803–819.

8 J. Sun, L. Guo, X. Sun, J. Zhang, L. Hou, L. Li, S. Yang and C. Yuan, One-Dimensional Nanostructured Pseudocapacitive Materials: Design, Synthesis and Applications in Supercapacitors, *Batteries Supercaps*, 2019, **2**, 820–841.

9 G. S. Vadehra, R. P. Maloney, M. A. Garcia-Garibay and B. Dunn, Naphthalene Diimide Based Materials with Adjustable Redox Potentials: Evaluation for Organic Lithium-Ion Batteries, *Chem. Mater.*, 2014, **26**, 7151–7157.

10 C. R. DeBlase, K. Hernandez-Burgos, J. M. Rotter, D. J. Fortman, S. Abreu Ddos, R. A. Timm, I. C. Diogenes, L. T. Kubota, H. D. Abruna and W. R. Dichtel, Cation-Dependent Stabilization of Electrogenerated Naphthalene Diimide Dianions in Porous Polymer Thin Films and Their Application to Electrical Energy Storage, *Angew. Chem., Int. Ed.*, 2015, **54**, 13225–13229.

11 S. K. Nalluri, Z. Liu, Y. Wu, K. R. Hermann, A. Samanta, D. J. Kim, M. D. Krzyaniak, M. R. Wasielewski and J. F. Stoddart, Chiral Redox-Active Isosceles Triangles, *J. Am. Chem. Soc.*, 2016, **138**, 5968–5977.

12 Z. Luo, L. Liu, Q. Zhao, F. Li and J. Chen, An Insoluble Benzoquinone-Based Organic Cathode for Use in Rechargeable Lithium-Ion Batteries, *Angew. Chem., Int. Ed.*, 2017, **56**, 12561–12565.

13 D. Yin, H. Zhao, N. Li, R. Si, X. Sun, X. Li and Y. Du, Enhancing the Rate Capability of Niobium Oxide Electrode through Rare-Earth Doping Engineering, *Batteries Supercaps*, 2019, **2**, 924–928.

14 Y. Cui, X. Zhou, W. Guo, Y. Liu, T. Li, Y. Fu and L. Zhu, Selenium Nanocomposite Cathode with Long Cycle Life for Rechargeable Lithium-Selenium Batteries, *Batteries Supercaps*, 2019, **2**, 784–791.

15 Z. Fang, J. Wang, H. Wu, Q. Li, S. Fan and J. Wang, Progress and challenges of flexible lithium ion batteries, *J. Power Sources*, 2020, **454**, 227932.

16 L. Yang, W. Wei, Y. Ma, Y. Xu and G. Chang, Intermolecular channel expansion induced by cation-π interactions to enhance lithium storage in a crosslinked π-conjugated organic anode, *J. Power Sources*, 2020, **449**, 227551.

17 Z. Guo, L. Chen, Y. Wang, C. Wang and Y. Xia, Aqueous Lithium-Ion Batteries Using Polyimide-Activated Carbon Composites Anode and Spinel LiMn2O4 Cathode, *ACS Sustainable Chem. Eng.*, 2017, **5**, 1503–1508.

18 M. Walter, K. V. Kravchyk, C. Bofer, R. Widmer and M. V. Kovalenko, Polypyrenes as High-Performance Cathode Materials for Aluminum Batteries, *Adv. Mater.*, 2018, **30**, 1705644.

19 Y. Ma, X. Dong, Y. Wang and Y. Xia, Decoupling Hydrogen and Oxygen Production in Acidic Water Electrolysis Using a Polytriphenylamine-Based Battery Electrode, *Angew. Chem., Int. Ed.*, 2018, **57**, 2904–2908.

20 C. Ma, L. Wu, Z. Jin, X.-Y. Zhao, Y.-S. Liu, Y.-L. Bai, H. Sun, K.-X. Wang and J.-S. Chen, Thiophene Derivative as a High Electrochemical Active Anode Material for Sodium-Ion Batteries: The Effect of Backbone Sulfur, *Chem. Mater.*, 2018, **30**, 8426–8430.

21 Y. Liang and Y. Yao, Positioning Organic Electrode Materials in the Battery Landscape, *Joule*, 2018, **2**, 1690–1706.

22 N. Casado, G. Hernandez, A. Veloso, S. Devaraj, D. Mecerreyes and M. Armand, PEDOT Radical Polymer with Synergetic Redox and Electrical Properties, *ACS Macro Lett.*, 2016, **5**, 59–64.

23 G. Li, B. Zhang, J. Wang, H. Zhao, W. Ma, L. Xu, W. Zhang, K. Zhou, Y. Du and G. He, Electrochromic Poly(chalcogenoviologen)s as Anode Materials for High-Performance Organic Radical Lithium-Ion Batteries, *Angew. Chem., Int. Ed.*, 2019, **58**, 8468–8473.

24 D. J. Kim, Y. H. Jung, K. K. Bharathi, S. H. Je, D. K. Kim, A. Coskun and J. W. Choi, An Aqueous Sodium Ion Hybrid Battery Incorporating an Organic Compound and a Prussian Blue Derivative, *Adv. Energy Mater.*, 2014, **4**, 1400133.

25 Q. Zhao, Z. Zhu and J. Chen, Molecular Engineering with Organic Carbonyl Electrode Materials for Advanced Stationary and Redox Flow Rechargeable Batteries, *Adv. Mater.*, 2017, **29**, 1607007.

26 H. C. Zhang, Y. P. Xie, X. J. Chen, T. Jia, W. R. Huang, S. L. Luo, Q. Hou, R. H. Zeng and Z. Q. Sun, Naphthalene Diimide-Ethylene Conjugated Copolymer as Cathode Material for Lithium Ion Batteries, *J. Electrochem. Soc.*, 2017, **164**, A290–A294.

27 B. Häupler, A. Wild and U. S. Schubert, Carbonyls: Powerful Organic Materials for Secondary Batteries, *Adv. Energy Mater.*, 2015, **5**, 1402034.

28 Z. Song, H. Zhan and Y. Zhou, Polyimides: promising energy-storage materials, *Angew. Chem., Int. Ed.*, 2010, **49**, 8444–8448.

29 F. Xu, J. Xia, W. Shi and S.-a. Cao, Sulfonyl-based polyimide cathode for lithium and sodium secondary batteries: enhancing the cycling performance by the electrolyte, *Mater. Chem. Phys.*, 2016, **169**, 192–197.

30 Y. Huang, K. Li, J. Liu, X. Zhong, X. Duan, I. Shakir and Y. Xu, Three-dimensional graphene/polyimide composite-derived flexible high-performance organic cathode for rechargeable lithium and sodium batteries, *J. Mater. Chem. A*, 2017, **5**, 2710–2716.

31 A. V. Mumyatov, A. F. Shestakov, N. N. Dremova, K. J. Stevenson and P. A. Troshin, New Naphthalene-Based Polyimide as an Environment-Friendly Organic Cathode Material for Lithium Batteries, *Energy Technol.*, 2019, **7**, 1801016.

32 H. Wu, K. Wang, Y. Meng, K. Lu and Z. Wei, An organic cathode material based on a polyimide/CNT nanocomposite for lithium ion batteries, *J. Mater. Chem. A*, 2013, **1**, 6366.

33 L. Chen, W. Li, Y. Wang, C. Wang and Y. Xia, Polyimide as anode electrode material for rechargeable sodium batteries, *RSC Adv.*, 2014, **4**, 25369–25373.

34 H.-g. Wang, S. Yuan, D.-l. Ma, X.-l. Huang, F.-l. Meng and X.-b. Zhang, Tailored Aromatic Carbonyl Derivative Polyimides for High-Power and Long-Cycle Sodium-Organic Batteries, *Adv. Energy Mater.*, 2014, **4**, 1301651.

 

35 H. Wu, Q. Meng, Q. Yang, M. Zhang, K. Lu and Z. Wei, Large-Area Polyimide/SWCNT Nanocable Cathode for Flexible Lithium-Ion Batteries, *Adv. Mater.*, 2015, **27**, 6504–6510.

36 A. Ahmad, H. Wu, Y. Guo, Q. Meng, Y. Meng, K. Lu, L. Liu and Z. Wei, A graphene supported polyimide nanocomposite as a high performance organic cathode material for lithium ion batteries, *RSC Adv.*, 2016, **6**, 33287–33294.

37 H. P. Wu, Q. Yang, Q. H. Meng, A. Ahmad, M. Zhang, L. Y. Zhu, Y. G. Liu and Z. X. Wei, A polyimide derivative containing different carbonyl groups for flexible lithium ion batteries, *J. Mater. Chem. A*, 2016, **4**, 2115–2121.

38 Y. Liang, Z. Chen, Y. Jing, Y. Rong, A. Facchetti and Y. Yao, Heavily n-Dopable pi-Conjugated Redox Polymers with Ultrafast Energy Storage Capability, *J. Am. Chem. Soc.*, 2015, **137**, 4956–4959.

39 Z. Li, J. Zhou, R. Xu, S. Liu, Y. Wang, P. Li, W. Wu and M. Wu, Synthesis of three dimensional extended conjugated polyimide and application as sodium-ion battery anode, *Chem. Eng. J.*, 2016, **287**, 516–522.

40 K. T. Sarang, A. Miranda, H. An, E.-S. Oh, R. Verduzco and J. L. Lutkenhaus, Poly(fluorene-alt-naphthalene diimide) as n-Type Polymer Electrodes for Energy Storage, *ACS Appl. Polym. Mater.*, 2019, **1**, 1155–1164.

41 Z. Wang, R. Song, Y. Zhang, T. Zhang, X. Zhu, J. Zeng, W. Zhang, Z. Zhao, N. Yan and G. He, Biphenyl Diimides-based Novel Blue Emitters with Aggregation Induced Blue-Shifted Emission Characteristics, *ChemPhotoChem*, 2020, **4**, 59–67.

42 Y. Kim, J. Hong, J. H. Oh and C. Yang, Naphthalene Diimide Incorporated Thiophene-Free Copolymers with Acene and Heteroacene Units: Comparison of Geometric Features and Electron-Donating Strength of Co-units, *Chem. Mater.*, 2013, **25**, 3251–3259.

43 H. Usta, G. Lu, A. Facchetti and T. J. Marks, Dithienosilole- and Dibenzosilole-Thiophene Copolymers as Semiconductors for Organic Thin-Film Transistors, *J. Am. Chem. Soc.*, 2006, **128**, 9034–9035.

44 N. Zhou, X. Guo, R. P. Ortiz, S. Li, S. Zhang, R. P. Chang, A. Facchetti and T. J. Marks, Bithiophene imide and benzodithiophene copolymers for efficient inverted polymer solar cells, *Adv. Mater.*, 2012, **24**, 2242–2248.

45 K. Kanosue, R. n. Augulis, D. Peckus, R. Karpicz, T. Tamulevičius, S. Tamulevičius, V. Gulbinas and S. Ando, Polyimide and Imide Compound Exhibiting Bright Red Fluorescence with Very Large Stokes Shifts *via* Excited-State Intramolecular Proton Transfer II. Ultrafast Proton Transfer Dynamics in the Excited State, *Macromolecules*, 2016, **49**, 1848–1857.

46 H. Zhao, J. Wang, Y. Zheng, J. Li, X. Han, G. He and Y. Du, Organic Thiocarboxylate Electrodes for a Room-Temperature Sodium-Ion Battery Delivering an Ultrahigh Capacity, *Angew. Chem., Int. Ed.*, 2017, **56**, 15334–15338.

47 A. R. Murphy, J. S. Liu, C. Luscombe, D. Kavulak, J. M. J. Frechet, R. J. Kline and M. D. McGehee, Synthesis, characterization, and field-effect transistor performance of carboxylate-functionalized polythiophenes with increased air stability, *Chem. Mater.*, 2005, **17**, 4892–4899.

48 J. Wang, H. Zhao, L. Xu, Y. Yang, G. He and Y. Du, Three-Electron Redox Enabled Dithiocarboxylate Electrode for Superior Lithium Storage Performance, *ACS Appl. Mater. Interfaces*, 2018, **10**, 35469–35476.